Mon. Not. R. Astron. Soc. **000**, 1–6 (2005) Printed 4 February 2008 (MN LATEX style file v2.2)

Separating out the Alcock-Paczyński Effect on 21cm Fluctuations

R. Barkana ⋆
School of Physics and Astronomy, The Raymond and Beverly Sackler Faculty of Exact Sciences, Tel Aviv University, Tel Aviv 69978, ISRAEL

4 February 2008

ABSTRACT
We reconsider the Alcock-Paczyński effect on 21cm fluctuations from high redshift, focusing on the 21cm power spectrum. We show that at each accessible redshift both the angular diameter distance and the Hubble constant can be determined from the power spectrum, at epochs and on scales where the ionized fraction fluctuations are linear. Furthermore, this is possible using anisotropies that depend only on linear density perturbations and not on astrophysical sources of 21cm fluctuations. We show that measuring these quantities at high redshift would not just confirm results from the cosmic microwave background; if the 21cm power spectrum can be measured to better than 10% precision, it will improve constraints from the CMB alone on cosmological parameters including dark energy.

Key words: galaxies:high-redshift – cosmology:theory – galaxies:formation

1 INTRODUCTION

Resonant absorption by neutral hydrogen at its spin-flip 21cm transition can be used to map its three-dimensional distribution at early cosmic times (Hogan & Rees 1979; Scott & Rees 1990; Madau et al. 1997). The primordial inhomogeneities in the cosmic gas induced variations in the optical depth for absorption of the cosmic microwave background (CMB) at the redshifted 21cm wavelength. Absorption occurs as long as the spin temperature of hydrogen, T_s (which characterizes the population ratio of the upper and lower states of the 21cm transition), is lower than the CMB temperature, T_γ. This condition is satisfied in the redshift interval $20 \lesssim z \lesssim 200$ (Loeb & Zaldarriaga 2004), before the first galaxies formed in the universe (Barkana & Loeb 2001), while 21cm emission is expected at later epochs.

Several groups are currently constructing low-frequency radio arrays capable of detecting the diffuse 21cm radiation; these include the *Primeval Structure Telescope* (web.phys.cmu.edu/∼past), the *Mileura Widefield Array* (web.haystack.mit.edu/arrays/MWA), and the *Low Frequency Array* (www.lofar.org). The 21cm measurements depend on the spin temperature T_s which itself depends on the kinetic gas temperature T_k and also on the strength of coupling between T_s and T_k, a coupling that is due to atomic collisions or to indirect coupling through Lyα radiation from the first stars (Wouthuysen 1952; Field 1958; Madau et al. 1997; Ciardi & Madau 2003). Fluctuations in these quantities are expected to produce isotropic 21cm fluctuations. Upcoming experiments are expected to successfully detect the 21cm fluctuations despite the required high sensitivity and the presence of strong foregrounds (Zaldarriaga et al. 2004; Santos et al. 2005; Bowman, Morales & Hewitt 2006).

Cosmological measurements generally determine three-dimensional locations indirectly, using angular position on the sky and redshift along the line of sight. This indirect route can modify any measured power spectrum and produce spurious anisotropies even when the underlying power spectrum is intrinsically isotropic. One such effect is that of redshift distortions, which appear when peculiar velocity gradients cause apparent changes in line-of-sight distances and thus in apparent densities. This effect has been studied extensively in galaxy redshift surveys (Kaiser 1987; Nusser & Davis 1994; Taylor & Hamilton 1996; Desjacques et al. 2004), where it can be used to probe a degenerate combination of the cosmic mean density of matter and galaxy bias. In the case of fluctuations in the 21cm brightness temperature relative to the CMB, the same effect (Bharadwaj & Ali 2004a,b) produces a line-of-sight anisotropy which is of great importance since it permits a separation of the physics from the astrophysics of 21cm fluctuations (Barkana & Loeb 2005a); i.e., it allows observers to measure fundamental cosmological parameters through the linear power spectrum, and to separately probe the effects of stellar and quasar radiation on the intergalactic medium.

A second anisotropy results if data are analyzed using assumed cosmological parameters that differ from the true ones. In this situation, separations along the line of sight

⋆ E-mail: barkana@wise.tau.ac.il

are scaled differently from those on the sky, and this distorts the appearance of any spherical object or isotropic statistical distribution. This creates a spurious anisotropy that the Alcock-Paczyński (AP) test exploits in order to constrain the cosmological parameters (Alcock & Paczyński 1979; Hui, Stebbins & Burles 1999).

Recently, Nusser (2005) suggested to apply the AP test to 21cm fluctuations from high redshift. Nusser (2005) considered 21cm fluctuations produced by density perturbations and neutral fraction fluctuations, as well as the anisotropies due to redshift distortions and the AP effect. Nusser (2005) showed that the correlation function (as a function of comoving position $\mathbf{r}$) has a portion $P_6(\mu_r)$ that appears only in the presence of AP anisotropy, where μ_r is the cosine of the angle between $\mathbf{r}$ and the line of sight, and P_6 is the $6^{\rm th}$-order Legender polynomial. Ali, Bharadwaj & Pandey (2005) also analyzed anisotropies in the clustering pattern of redshifted 21cm maps. They considered the same anisotropy sources as Nusser (2005) and showed that the anisotropy is affected both by the H I distribution and by cosmological parameters, making it hard to disentangle the AP effect; however, they did not include the $P_6(\mu_r)$ term but only considered lower-order terms.

In this paper we reconsider the AP effect on 21cm fluctuations from high redshift. Our analysis is valid even in the presence of the whole gamut of possible sources of 21cm fluctuations: isotropic fluctuations in gas density, Lyα flux (Barkana & Loeb 2005b), neutral fraction, and temperature, as well as the velocity gradient anisotropy and the AP effect. We do not assume that these sources produce fluctuations that are proportional to density fluctuations, we do not neglect temperature fluctuations, and we also do not assume the Einstein-de Sitter growing mode when calculating the redshift distortions; instead, we apply exact linear perturbation theory at high redshifts, including the effects of the CMB and the difference in the evolution of the dark matter and the baryons (Barkana & Loeb 2005c; Naoz & Barkana 2005). At lower redshifts, when the first galaxies produce Lyα , UV, and X-ray photons, we assume only that the 21cm fluctuations remain small and can be treated to linear order. Fluctuations that are due to optically thin radiation backgrounds are expected to indeed be small, since any given gas parcel encounters radiation that is averaged over sources distributed in a large surrounding region, leading to linear fluctuations as in the case of Lyα flux (Barkana & Loeb 2005b). Thus our results are valid at high redshift before the formation of the first galaxies, and later during Lyα coupling and X-ray heating. Such a regime of observable 21cm fluctuations before reionization is indeed expected theoretically (Madau et al. 1997; Sethi 2005; Furlanetto 2006).

During reionization, our results are valid if X-rays reionized the universe (Oh 2001; Madau et al. 2004). Stellar UV photons instead produce sharply-defined H II regions, but in this case the neutral fraction fluctuations may still be small on large enough scales, especially early in reionization, when the cosmic mean neutral fraction is still much smaller than unity. There are several difficulties, however. Once reionization begins in earnest, comoving scales well above 10 Mpc may be required in order to exceed the typical size of ionized bubbles (Barkana & Loeb 2004; Furlanetto, Zaldarriaga, & Hernquist 2004). On such large scales, the correlations are relatively weak and thus harder to observe, and also the delay due to the light travel time along the line of sight produces a significant additional anisotropy on such scales (McQuinn et al. 2006; Barkana & Loeb 2006).

Unlike previous studies of the AP effect we focus on the 21cm power spectrum, a quantity which is much closer to the observable radio visibilities. We first consider the AP effect on power spectra in general (§ 2), and then show that the 21cm power spectrum allows for a simple separation of the AP anisotropy from other effects, as well as a separate measurement of the Hubble constant at high redshift (§ 3). We show that the appropriate power spectrum coefficients are large enough to be feasible to measure (§ 4.1), and the measured quantities yield extra cosmological information beyond CMB measurements (§ 4.2). We summarize our results in § 5.

2 THE AP EFFECT ON THE POWER SPECTRUM

An incorrect choice of cosmological parameters in the analysis of cosmological data scales both the angular and line-of-sight coordinates. We denote the angular distance out to z as D_A, and the Hubble constant at z as H. Following Nusser (2005), we define $(1+\alpha)$ as the ratio of the true value of HD_A to its assumed value. This quantity depends on the ratio between the line-of-sight and angular scales, and thus introduces anisotropy in the power spectrum and corresponds to the classical AP test. However, even a redshift-dependent overall scaling of the coordinates (i.e., with $\alpha = 0$) may have observable effects on the power spectrum, as discussed below. Thus, we also define $(1+\alpha_\perp)$ as the same ratio but for D_A rather than for the quantity HD_A. This implies that any assumed angular distance equals $1/(1+\alpha_\perp)$ times the true distance, and any assumed line-of-sight distance equals $(1+\alpha)/(1+\alpha_\perp)$ times the true one. Overall, we refer to these various scalings simply as the AP effect.

Suppose we observe the relative fluctuation δ in some underlying field (which may be the density of some component or the 21cm brightness temperature T_b). Then if we observe δ at a comoving position $\mathbf{r}$ (typically measured in Mpc) with coordinates (x_c, y_c, z_c), where $\mathbf{r}$ is reconstructed from the angular position and redshift using the assumed cosmology, we actually detect δ at a true comoving position $\mathbf{r}^{\rm tr}$ with coordinates

$$\mathbf{r}^{\rm tr} = \left((1+\alpha_\perp)x_c, (1+\alpha_\perp)y_c, \frac{1+\alpha_\perp}{1+\alpha} z_c\right) \ . \tag{1}$$

If the Fourier transform of $\delta(\mathbf{r}^{\rm tr})$ with respect to $\mathbf{r}^{\rm tr}$ (i.e., in the absence of the AP effect) is $\tilde{\delta}^{\rm tr}(\mathbf{k})$, where the comoving wavevector $\mathbf{k}$ has coordinates (k_x, k_y, k_z), then the observed Fourier transform of $\delta(\mathbf{r})$ with respect to $\mathbf{r}$ is

$$\tilde{\delta}(\mathbf{k}) = \frac{1+\alpha}{(1+\alpha_\perp)^3} \tilde{\delta}^{\rm tr}(\mathbf{k}^{\rm tr}) \ , \tag{2}$$

where we have defined

$$\mathbf{k}^{\rm tr} \equiv \left(\frac{1}{1+\alpha_\perp} k_x, \frac{1}{1+\alpha_\perp} k_y, \frac{1+\alpha}{1+\alpha_\perp} k_z\right) \ . \tag{3}$$

Using the definition of the power spectrum in terms of an ensemble average and a Dirac delta function, we define power spectra $P(\mathbf{k})$ and $P^{\rm tr}(\mathbf{k})$ as

$$\langle\tilde{\delta}(\mathbf{k}_1)\tilde{\delta}(\mathbf{k}_2)\rangle = (2\pi)^3\delta^D(\mathbf{k}_1+\mathbf{k}_2)P(\mathbf{k}_1)\ , \quad (4)$$

and

$$\langle\tilde{\delta}^{\rm tr}(\mathbf{k}_1)\tilde{\delta}^{\rm tr}(\mathbf{k}_2)\rangle = (2\pi)^3\delta^D(\mathbf{k}_1+\mathbf{k}_2)P^{\rm tr}(\mathbf{k}_1)\ , \quad (5)$$

respectively. We then find that the AP effect distorts the observed power spectrum of δ compared with the true one:

$$P(\mathbf{k}) = \frac{1+\alpha}{(1+\alpha_\perp)^3}P^{\rm tr}(\mathbf{k}^{\rm tr})\ . \quad (6)$$

We now specialize to an underlying power spectrum of the form $P^{\rm tr}(k^{\rm tr},\mu^{\rm tr})$ where $\mu^{\rm tr}=k_z^{\rm tr}/k^{\rm tr}$ is the cosine of the angle between the $\mathbf{k}$ vector and the line of sight; thus, we assume a power spectrum with a line-of-sight anisotropy only. We also expand to first order in the corrections α and $\alpha_\perp$. Then using the relations

$$\frac{k^{\rm tr}}{k} = 1+\alpha\mu^2-\alpha_\perp\ ;\quad \frac{\mu^{\rm tr}}{\mu} = 1+\alpha(1-\mu^2)\ , \quad (7)$$

we obtain

$$\begin{aligned} P(k,\mu) &= (1+\alpha-3\alpha_\perp)P^{\rm tr} + (\alpha\mu^2-\alpha_\perp)\frac{\partial P^{\rm tr}}{\partial\log k} \quad (8)\\ &\quad +\alpha(1-\mu^2)\frac{\partial P^{\rm tr}}{\partial\log\mu}\ , \end{aligned}$$

where henceforth $P^{\rm tr}$ with no explicit argument is evaluated at the *observed* $\mathbf{k}$.

3 THE CASE OF THE 21CM POWER SPECTRUM

We assume a flat universe with cosmological parameters (Spergel et al. 2003) $h=0.72$, $\Omega_m=0.27$, and $\Omega_r = 8.0\times10^{-5}$ (assuming 3 massless neutrinos), with the remaining energy density in a cosmological constant. Then the mean brightness temperature offset on the sky at redshift z is (Madau et al. 1997)

$$\begin{aligned} T_b &= 4.74\,{\rm mK}\left[\frac{(1+z)^2}{H(z)/H_0}\right]\left(\frac{\Omega_b h}{.033}\right)\left(\frac{T_s-T_\gamma}{T_s}\right) \quad (9)\\ &\simeq 28.8\,{\rm mK}\left(\frac{\Omega_b h}{.033}\right)\left(\frac{\Omega_m}{.27}\right)^{-\frac{1}{2}}\left(\frac{1+z}{10}\right)^{\frac{1}{2}}\left(\frac{T_s-T_\gamma}{T_s}\right)\ , \end{aligned}$$

where the second expression is accurate to 1% at $4\lesssim z\lesssim 70$ (where the contributions of both vacuum energy and radiation can be neglected).

Since fluctuations in the 21cm brightness temperature are produced by various isotropic sources plus the line-of-sight velocity gradients, the linear power spectrum (in the absence of the AP effect) can be written in the form (Barkana & Loeb 2005a)

$$P^{\rm tr}_{T_b}(\mathbf{k}) = \mu^4 P^{\rm tr}_{\mu^4}(k) + \mu^2 P^{\rm tr}_{\mu^2}(k) + P^{\rm tr}_{\mu^0}(k)\ . \quad (10)$$

While $P^{\rm tr}_{\mu^0}$ and $P^{\rm tr}_{\mu^2}$ depend not only on fluctuations in the gas density and temperature but also on stellar radiation fields, $P^{\rm tr}_{\mu^4}(k)$ is due to velocity gradients and is always the power spectrum of $\dot{\delta}_b H^{-1}$, where $\dot{\delta}_b$ is the time derivative of the baryon density.

To calculate the AP effect in this case we apply Eq. (8) and find a modified 21cm power spectrum:

$$P_{T_b}(\mathbf{k}) = \mu^6 P_{\mu^6}(k) + \mu^4 P_{\mu^4}(k) + \mu^2 P_{\mu^2}(k) + P_{\mu^0}(k)\ , \quad (11)$$

where

$$\begin{aligned} P_{\mu^6} &= -\alpha\left(4P^{\rm tr}_{\mu^4} - \frac{\partial P^{\rm tr}_{\mu^4}}{\partial\log k}\right)\ ;\\ P_{\mu^4} &= P^{\rm tr}_{\mu^4} + \alpha\left(5P^{\rm tr}_{\mu^4} - 2P^{\rm tr}_{\mu^2} + \frac{\partial P^{\rm tr}_{\mu^2}}{\partial\log k}\right)\\ &\quad -\alpha_\perp\left(3P^{\rm tr}_{\mu^4} + \frac{\partial P^{\rm tr}_{\mu^4}}{\partial\log k}\right)\ ; \quad (12)\\ P_{\mu^2} &= P^{\rm tr}_{\mu^2} + \alpha\left(3P^{\rm tr}_{\mu^2} + \frac{\partial P^{\rm tr}_{\mu^0}}{\partial\log k}\right) - \alpha_\perp\left(3P^{\rm tr}_{\mu^2} + \frac{\partial P^{\rm tr}_{\mu^2}}{\partial\log k}\right)\ ;\\ P_{\mu^0} &= (1+\alpha)P^{\rm tr}_{\mu^0} - \alpha_\perp\left(3P^{\rm tr}_{\mu^0} + \frac{\partial P^{\rm tr}_{\mu^0}}{\partial\log k}\right)\ . \end{aligned}$$

First of all, the AP effect changes the three observable isotropic power spectra, P_{μ^4}, P_{μ^2}, and P_{μ^0}. The effect of an overall scaling (i.e., non-zero $\alpha_\perp$) is to distort the shape and normalization of each of these power spectra. On the other hand, the parameter α corresponds to an anisotropy, and it mixes the different power spectra. In particular, $P^{\rm tr}_{\mu^4}(k)$ now gets a correction of order α that can depend on stellar radiation. However, the velocity distortion and AP anisotropies also combine to produce a fourth observable power spectrum, P_{μ^6} [analogous to the P_6 term in the correlation function (Nusser 2005)]. The k-dependence of this term depends on linear perturbation theory only, and the term is not zero since the power spectrum of density fluctuations has a logarithmic slope well below 4 on all scales. Thus, the new P_{μ^6} term is a direct probe of the AP anisotropy parameter α. Its coefficient, though, depends on the linear power spectrum which is itself a function of the unknown cosmological parameters.

If we assume that the shape of the primordial power spectrum from inflation can be described with a few parameters (e.g., with a power law index plus its first derivative with respect to k), then these parameters can be reconstructed at the same time as the cosmological parameters in an iterative procedure. After the first measurement of α is made at a given redshift, the cosmological parameters can be adjusted to give the right value of HD_A at that redshift. A re-analysis of the data with the new cosmological parameters should yield a new α that is close to zero, but not exactly, since changing the parameters changes the k-dependent coefficient of α. The procedure can be iterated until α converges very close to zero. At this point, P_{μ^4} allows a measurement of $\alpha_\perp$ from the predicted shape of $P^{\rm tr}_{\mu^4}$. Again, the measurement can be iterated until cosmological parameters are found such that the 21cm power spectrum is consistent with both α and $\alpha_\perp$ equal to zero.

This procedure is made easier by observing the 21cm power spectrum (and thus the coefficients of α and $\alpha_\perp$) at a range of values of k and at a range of redshifts, since the k and z dependence of these terms is precisely known for given cosmological parameters. Since the number of parameters in the standard cosmological models is relatively small, a large number of measured points should help overcome degeneracies as well as difficulties with noise and foregrounds. The determination of the parameters may be helped by the presence of distinct features in $P^{\rm tr}_{\mu^4}$, specifically the signatures of the acoustic oscillations on large scales (see § 4.2). Note that any change of $\alpha_\perp$ with redshift further helps to

separate it from uncertainties in the shape of the power spectrum, since the redshift dependence of the power spectrum itself is known theoretically. The redshift variation of $\alpha_\perp$ is however fairly weak, e.g., if a 10% overestimate of Ω_m is used in the analysis, then $\alpha_\perp = 3.3\%$ at redshift 7, 3.5% at $z = 10$, 3.6% at $z = 20$, and 3.8% at $z = 100$.

4 IMPLICATIONS

4.1 Power spectra

As noted in the previous section, the AP effect allows α and $\alpha_\perp$ to be measured from observations of 21cm fluctuations, and once they are measured at a given redshift, a reanalysis with parameters that set $\alpha = \alpha_\perp = 0$ can be used to recover the three true underlying power spectra. The analysis is particularly simple at high redshift, before the first galaxies formed (but at $z < 150$), on large-scale structure scales (i.e., k between 0.01 and 40 Mpc^{-1}). Barkana & Loeb (2005c) showed that in this regime the 21cm power spectra at various redshifts can be described as linear combinations of five fixed initial fluctuation modes (i.e., functions of k), with redshift-dependent coefficients. Neglecting the AP effect, they argued that the five modes and the linear coefficients can all be determined directly from observations. Specifically, if the three observable power spectra are measured at N k-values at M different redshifts, then there are a total of $3NM$ data points. Modeling the data in terms of the amplitudes of the five modes at the same N k-values, along with two coefficients per redshift for each mode [see Barkana & Loeb (2005c) for details], yields a total of $5N + 10M$ parameters. In this case, $M = 2$ redshifts suffice to determine all the parameters as long as $N \geqslant 20$.

Now we consider adding to this the AP effect, within the theoretical framework presented in the previous section but without assuming a theoretical calculation of the modes or the redshift coefficients. We thus add the two AP parameters per redshift, and the derivatives with respect to $\log k$ of the five modes [see Eq. (12)], for a total of $10N + 12M$ parameters. This must be compared with $4NM$ data points, where we have included the μ^6 term at each k and z. In this case, obtaining at least as many data points as parameters requires $M = 4$ redshifts if $N \geqslant 8$, while $M = 3$ redshifts suffice if $N \geqslant 18$. Measurements at additional redshifts or at more values of k will allow a more accurate reconstruction along with multiple consistency checks.

Of more general interest are the two quantities involved in the determination of α and $\alpha_\perp$ at any redshift, even when reionization and other complex processes are underway. The first is the coefficient of α in P_{μ^6} in Eq. (12), which can be used to determine α. The second is the coefficient of $\alpha_\perp$ in P_{μ^4} in Eq. (12), which can be used to determine $\alpha_\perp$ after α has been zeroed. Figure 1 shows $P^{\rm tr}_{\mu^4}$ and these two coefficients at high redshifts (in brightness temperature units), assuming that galaxies have not yet formed and using the concordance cosmological parameters. Note that the signature of the large-scale acoustic oscillations in the power spectrum $P^{\rm tr}_{\mu^4}$ is magnified in its derivative $\partial_{\log k} P^{\rm tr}_{\mu^4}$ and therefore in the two coefficients. At some lower redshift, stellar radiation is expected to heat the gas well above the CMB through X-rays and to fully couple the spin temperature

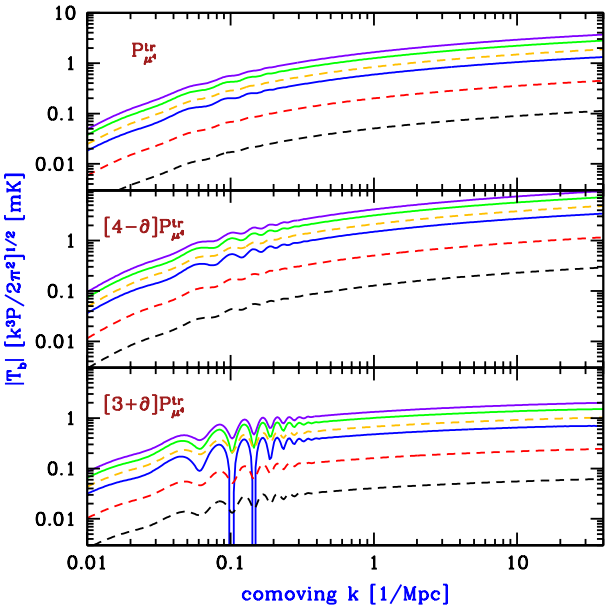

Figure 1. Power spectrum coefficients of 21cm brightness fluctuations versus wavenumber. We show the quantity $|T_b|[k^3P/(2\pi^2)]^{1/2}$, where P is replaced by $P^{\rm tr}_{\mu^4}$ (upper panel), $[4-\partial_{\log k}]P^{\rm tr}_{\mu^4}$ (middle panel), or $[3+\partial_{\log k}]P^{\rm tr}_{\mu^4}$ (lower panel). In each case we consider redshifts 150, 100, 50 (solid curves, from bottom to top), 35, 25, and 20 (dashed curves, from top to bottom), assuming no stellar radiation is present.

to the gas temperature indirectly through Lyα photons; although there are large uncertainties, projections of the properties of high-redshift galaxies suggest that heating and spin coupling are likely to occur well before cosmic reionization (Madau et al. 1997; Sethi 2005; Furlanetto 2006). Figure 2 shows $P^{\rm tr}_{\mu^4}$ and the same two coefficients at lower redshifts assuming that $T_s \gg T_\gamma$ due to stellar radiation. When considering the magnitudes of these terms, it is important to note the spherical averages $\langle\mu^4\rangle = 1/5$ and $\langle\mu^6\rangle = 1/7$, although the sensitivity of upcoming radio arrays may not be isotropic.

4.2 Cosmological parameters

CMB measurements (Spergel et al. 2003) have provided a precise determination of features in the linear power spectrum, including the matter-radiation turnover and the signature of the acoustic oscillations of the baryon-photon fluid. These features measure the properties of the various cosmic fluids at recombination, when dark energy (or a cosmological constant) was negligible. However, the observed angular scale subtended by these features provides a precise measurement of the angular diameter distance D_A to the epoch of recombination, an integrated quantity that is affected by dark energy at low redshift. The signatures of the acoustic oscillations have also been detected recently in the large-scale distribution of massive galaxies at $z \sim 0.35$ (Eisenstein et al. 2005; Cole et al. 2005). Upcoming larger redshift surveys out to $z \sim 1$ will begin to constrain significantly the properties of dark energy (Hu & Haiman 2003), although the precise constraint depends on prior assump-

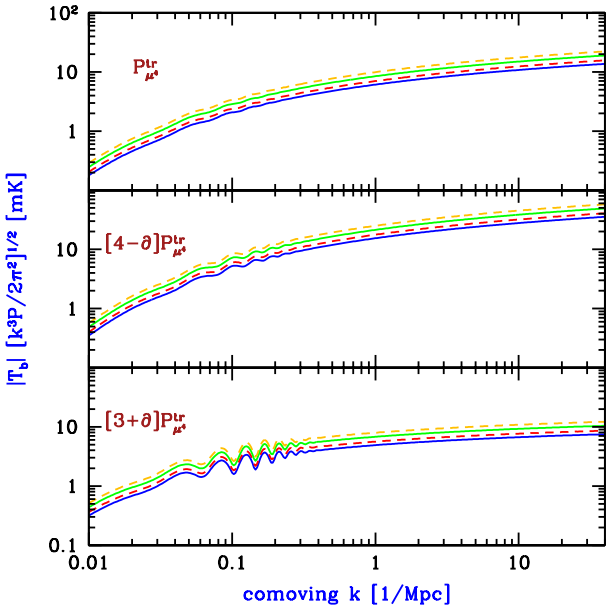

Figure 2. Power spectrum coefficients of 21cm brightness fluctuations versus wavenumber. Same as Figure 1, except that we assume that $T_s \gg T_\gamma$, and we consider in each case redshifts 20, 15, 10, and 7 (from bottom to top).

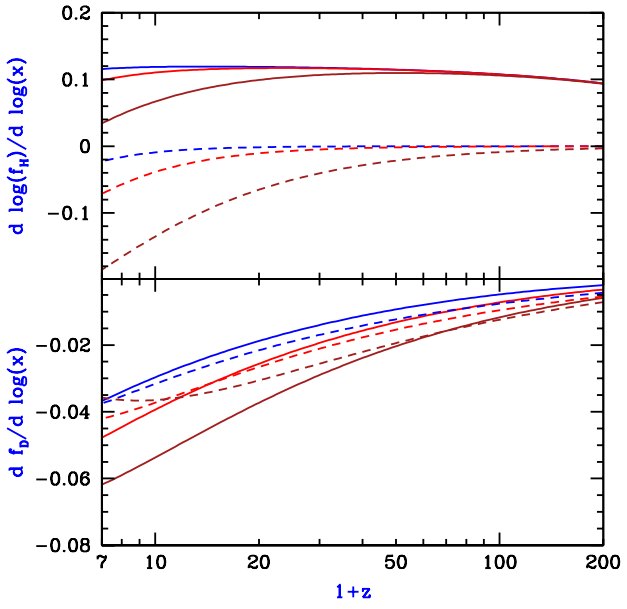

Figure 3. Relative sensitivity of $\log f_H(a)$ and $f_D(a)$ to cosmological parameters. For variations in a parameter x, we show $d/d\log(x)$ of $\log f_H$ (top panel) and of f_D (bottom panel). In each case we consider variations in Ω_m (solid curves) and in w (dashed curves). When we vary each parameter we fix the other one, and the variations are all carried out with respect to the Ω values given in the text, in a flat $\Omega_{\rm total} = 1$ universe, for $w = -1$, -0.75, and -0.5 (from top to bottom in each set of curves at $z = 20$).

tions on the possible complexity of the properties of dark energy (Maor et al. 2002).

We now consider the role that 21cm measurements can play in the general campaign to nail down the cosmological parameters and the properties of dark energy. As shown above, the AP effect on the 21cm power spectrum allows a direct measurement of α and $\alpha_\perp$, or equivalently of H and of D_A, at applicable redshifts. In this section we generalize to a flat universe with the energy density Ω_w (which remains after accounting for matter and radiation) consisting of a dark energy component with a constant equation of state $p = w\rho$. We also assume cosmic recombination (decoupling) at $a_{\rm rec} = 1/1090$ (Spergel et al. 2003), where $a = 1/(1+z)$ is the scale factor. Then the Hubble constant at scale factor a is

$$H(a) = H_0 \left[\Omega_m a^{-3} + \Omega_r a^{-4} + \Omega_w a^{-3(1+w)}\right]^{\frac{1}{2}} , \qquad (13)$$

and the angular diameter distance from redshift zero is

$$D_A(a) = a \int_a^1 \frac{da'}{a'^2 H(a')} . \qquad (14)$$

Although $D_A(a)$ at high redshift is sensitive to the value of w, this sensitivity is for the most part due to the low-redshift portion of the integral in Eq. (14). Thus, the sensitivity is substantially the same as that of $D_A(a_{\rm rec})$ which is measured from the CMB. So in order to accurately assess the ability of 21cm measurements to contribute cosmological information beyond the CMB, we consider the following fractional quantities:

$$f_H(a) \equiv \frac{H(a)}{H(a_{\rm rec})} \; ; \quad f_D(a) \equiv \frac{D_A(a_{\rm rec}) - \frac{a_{\rm rec}}{a} D_A(a)}{D_A(a_{\rm rec})} . \qquad (15)$$

We consider derivatives of $\log f_H$ (i.e., fractional changes in f_H), since $f_H \ll 1$ simply means that $H(a) \ll H(a_{\rm rec})$ and this does not represent a loss of precision. On the other hand, we consider derivatives of f_D, since $D_A(a) \simeq D_A(a_{\rm rec})$, and $f_D \ll 1$ represents a real loss of precision in the subtraction in the numerator of f_D.

Figure 3 shows the dependence of $\log f_H$ and of f_D on cosmological parameters, through their derivatives with respect to $\log \Omega_m$ (in a flat universe with fixed Ω_r), and with respect to $\log w$, both as a function of $1+z$, for various values of w with the Ω values as given above. The relative sensitivity to Ω_m is around 10% for $\log f_H$ and 4–6% (at the low-redshift end) for f_D. The relative sensitivity to w is significant only at the low redshift end ($z \sim 6$), where it is $\sim 4\%$ for f_D and between 2% (if $w = -1$) and 20% (if $w = -0.5$) for $\log f_H$.

5 SUMMARY

We have analyzed the AP effect on the power spectrum of 21cm fluctuations at high redshift. Including various sources of 21cm fluctuations, and assuming only that the fluctuations in the ionized fraction are linear, we have shown that the AP effect produces an anisotropic μ^6 term that can be used to measure and eliminate the AP anisotropy parameter α. This leaves a contribution to the μ^4 term that can be used to measure and eliminate the second AP parameter, $\alpha_\perp$. Both these AP terms depend only on linear density perturbations and not on 21cm fluctuations due to astrophysical sources that are far more uncertain. Measuring the angular diameter distance and the Hubble constant at high redshift (using α and $\alpha_\perp$) would provide constraints on Ω_m

and w. Assuming the same cosmological quantities are also measured at cosmic recombination from the CMB, the 21cm measurements maintain a relative sensitivity of order 10% to the cosmological parameters even after the common dependence with the CMB is eliminated. The planned 21cm experiments (see § 1) are expected to reach a brightness temperature sensitivity $\lesssim 1$ mK at $z \sim 10$, assuming that the foregrounds can be removed effectively; observations at higher redshifts will be much harder since the foreground emission increases approximately as $(1+z)^{2.5}$.

ACKNOWLEDGMENTS

The author acknowledges support by NSF grant AST-0204514 and Israel Science Foundation grant 28/02/01.

REFERENCES

Alcock, C., & Paczyński, B. 1979, Nature, 281, 358
Ali, S. S., Bharadwaj, S., & Pandey, B. 2005, MNRAS, 363, 251
Barkana, R., & Loeb, A. 2001, Phys. Rep., 349, 125
————————-. 2004, ApJ, 609, 474
————————-. 2005a, ApJ, 624, L65
————————-. 2005b, ApJ, 626, 1
————————-. 2005c, MNRAS, 363, L36
————————-. 2006, MNRAS Lett., in press (astro-ph/0512453)
Bharadwaj, S., & Ali, S. S. 2004a, MNRAS, 352, 142
Bharadwaj, S., & Ali, S. S. 2004b, MNRAS, 356, 1519
Bowman, J. D., Morales, M. F., & Hewitt, J. N. 2006, ApJ, 638, 20
Ciardi, B. & Madau, P. 2003, ApJ, 596, 1
Cole, S., et al. 2005, MNRAS, 362, 505
Desjacques, V., Nusser, A., Haehnelt, M. G., & Stoehr, F. 2004, MNRAS, 350, 879
Eisenstein, D., et al. 2005, ApJ, 633, 560
Field, G. B. 1958, Proc. IRE, 46, 240
Furlanetto, S. R. 2006, MNRAS, submitted [astro-ph/0604040]
Furlanetto, S. R., Zaldarriaga, M., Hernquist, L., 2004, ApJ, 613, 1
Hogan, C. J., & Rees, M. J. 1979, MNRAS, 188, 791
Hu, W., & Haiman, Z. 2003, Phys. Rev. D, 68, 063004
Hui, L., Stebbins, A., & Burles, S. 1999, ApJ, 511, 5
Kaiser, N. 1987, MNRAS, 227, 1
Loeb, A., & Zaldarriaga, M. 2004, Phys. Rev. Lett., 92, 211301
Madau, P., Meiksin, A., & Rees, M. J. 1997, ApJ, 475, 429
Madau P., Rees M. J., Volonteri M., Haardt F., Oh S. P., 2004, ApJ, 604, 484
Maor, I., Brustein, R., McMahon, J., & Steinhardt, P. J. 2002, Phys. Rev. D, 65, 123003
McQuinn, M., Zahn, O., Zaldarriaga, M., Hernquist, L., & Furlanetto, S. R. 2006, ApJ, submitted; astro-ph/0512263
Naoz, S., & Barkana, R. 2005, MNRAS, 362, 1047
Nusser, A. 2005, MNRAS, 364, 743
Nusser, A., & Davis, M. 1994, ApJ, 421
Oh S. P., 2001, ApJ, 553, 499
Santos, M. G., Cooray, A., & Knox, L. 2005, ApJ, 625, 575
Scott, D. & Rees, M. J. 1990, MNRAS, 247, 510
Sethi, S. K. 2005, MNRAS, 363, 818
Spergel, D. N., et al. 2003, ApJ, 148, 175
Taylor, A. N., & Hamilton, A. J. S. 1996, MNRAS, 282, 767
Wouthuysen, S. A., 1952, AJ, 57, 31
Zaldarriaga, M., Furlanetto, S. R., & Hernquist, L. 2004, ApJ, 608, 622

This paper has been typeset from a TEX/ LATEX file prepared by the author.